AISTech 2019 — Proceedings of the Iron & Steel Technology Conference
6–9 May 2019, Pittsburgh, Pa., USA
DOI 10.1000.377.213

Investigating Centerline Bridging in Continuous Casting During Speed Drops With ConOffline

Zhelin Chen[1], William Drennan[1], Brian G. Thomas[2], Joseph Bentsman[1]

[1]University of Illinois at Urbana-Champaign
1206 W Green St, Urbana, IL, USA, 61801
Phone: 217-418-4714
Email: zchen61@illinois.edu

[2]Colorado School of Mines
1610 Illinois St, Golden, CO, USA, 80401

Keywords: continuous casting, solidification, spray-cooling control, bridging, segregation

INTRODUCTION

Centerline segregation is a form of macrosegregation that appears in continuous-cast slabs as a region of impurities, usually accompanied by porosity, inclusions, alloy-rich regions, and even cracks, distributed near the centerline along the slab length [1]. These centerline defects are often very harmful to product quality, especially in highly-alloyed, segregation-prone steels, or when the slab is rolled into thin plates [1]. It is known that centerline segregation in continuous casting is related to bulging between rolls, bridging across uneven regions of the solidification front, and molten steel fluidity between the dendrites during the last stages of solidification [2].

Bridging refers to the phenomenon where the dendritic solidification fronts growing from opposite sides of the strand wide faces meet at some location upstream of the final metallurgical length, and thereby isolate a liquid pocket downstream. This pocket is surrounded by solid steel on all sides, so its shrinkage cannot be fed by the molten steel pool when it solidifies. Thus, the isolated liquid pocket solidifies like the center of a cast ingot, which usually results in high segregation, shrinkage cavities, porosity, and other centerline defects. Indeed, this slab-casting phenomenon is sometimes referred to as "mini-ingotism" [3]. Bridging has been shown to increase centerline segregation, because center-line segregation can be created by suction of alloy-rich liquid steel between the dendrites around the bridging region, due to the solidification shrinkage of the isolated liquid pocket [4]. One type of bridging is periodic bridging, a phenomenon thought to result from the periodic buildup of internal equiaxed grains settling down onto the outer radius of the strand's liquid core [5]. However, in this study, a mechanism for non-periodic bridging is investigated.

This paper identifies an important new mechanism for the formation of centerline bridging, due to sudden drops in casting speed, under spray table control within both thin and thick steel slab casters. Such sudden speed drops commonly accompany sticker-breakout alarms. The dynamic solidification heat-transfer model of the continuous casting process, ConOffline, is used to investigate this phenomenon. This model is an off-line version of CONONLINE [6], based on CON1D [7] that has been successfully used in previous work [8]–[13]. First, a brief introduction to the model is given. Then an example of bridging during a speed drop under spray table control is given, and a new mechanism for bridging is proposed. Finally, parametric studies are performed to investigate this new bridging phenomenon using the ConOffline model.

MODEL DESCRIPTION

ConOffline is a computational model of transient heat conduction and solidification during the entire continuous casting process, including the mold and strand. This model is an off-line version of the CONONLINE model, which has been implemented into a commercial caster for many years [14] and is described in detail elsewhere [5]. ConOffline uses recorded or specific history of casting conditions as inputs and can be used to perform numerical experiments that would be expensive, dangerous, or impossible on real caster. Furthermore, the conditions can be designed systematically and controlled precisely. Also, ConOffline can produce outputs that cannot be measured practically, such as the internal temperature distribution and the metallurgical length [14]. ConOffline has been used to investigate the transient evolution of the shell thickness profile during casting conditions changes [8-9].

1-D heat transfer model

For a solidifying steel strand with internal heat transfer occurring by conduction and advection, the temperature distribution is governed by the following equation of energy conservation:

$$\rho c_p^* \left(\frac{\partial T}{\partial t} + \vec{v} \cdot \nabla T \right) = \nabla \cdot \left(k \nabla T \right) \tag{1}$$

The strand moves in the casting direction at casting speed, v_c. Casting speeds are typically high enough to render axial heat conduction negligible relative to advection, as indicated by the high Peclet number of the process [7]. Furthermore, conduction in the width direction only matters near the corners of the slab. This enables simplifying the domain to a transverse slice through the strand thickness that spans from the shell surface at the inner radius to the outer radius surface, which moves with the steel in the casting direction at the casting speed. In this Lagrangian reference frame, equation (1) simplifies to

$$\rho c_p^* \frac{\partial T}{\partial t} = \frac{\partial}{\partial x} \left(k \frac{\partial T}{\partial x} \right) \tag{2}$$

where $T(x,t)$ is the temperature at any given point in the steel strand. The density ρ, thermal conductivity k, and effective specific heat c_p^* are temperature-dependent properties of the steel. The effective specific heat includes the latent heat of solidification,

$$c_p^* = c_p + L_f \frac{df_s}{dT} \tag{3}$$

where c_p is the usual specific heat, L_f is the latent heat of solidification, and f_s is the fraction of the steel that is solid at a given temperature.

The heat flux removed from boundary surfaces is assumed to be the same on either side of the strand for simplicity. The initial temperature of the steel is at the pouring temperature at the meniscus. In the mold, heat is removed from the surface according to a heat flux profile based on plant measurements [15], while below the mold in secondary cooling, heat is removed by natural convection, radiation, spray water hitting the surface, and contact with the containment rolls, which is discussed in detail in [6].

Heat flux in the mold depends on many complicated phenomena. In this work, average mold heat flux was taken as a function of casting speed, based on an empirical correlation for a thin slab caster developed previously [15]:

$$\bar{q}_m \left[\mathrm{MW/m^2} \right] = 1.197 \left(v_c \left[\mathrm{m/min} \right] \right)^{0.544} \tag{4}$$

For heat flux in the secondary cooling region, Nozaki's empirical correlation [16] was used for the spray cooling regions:

$$q_{sw} = 0.3925 \cdot Q_{sw}^{0.55} \cdot \left(1 - 0.0075 \cdot T_{sw} \right) \tag{5}$$

where T_{sw} and Q_{sw} are temperature of the cooling water spray and the spray water flux in $L/m^2/min$ of the spray water hitting the steel at that point on the surface. Heat transfer during secondary cooling is a subject of ongoing research, and other relations are available and used at different casters.

Dynamic model by delay interpolation

Equation (2) can be solved faster than real-time, but it only calculates the temperature within a single slice at the location of the moving reference frame based on the given casting speed history. To obtain the complete temperature distribution in the entire strand, as it evolves in time, ConOffline manages the simulation of *N* different slices simultaneously. Each slice starts at the meniscus at a different time to achieve a fixed *z*-distance spacing in between slices. For the i^{th} slice starting at the meniscus at time t_0^i, the solution to equation (2) for this slice is $T_i(x,t)$. Mathematically, this is expressed as:

$$T\left(x, z_i(t), t\right) = T_i(x,t) \tag{6}$$

where

$$z_i(t) = \int_{t_0^i}^{t} v_c \, dt \tag{7}$$

Which is the location of the i^{th} slice below the meniscus at time t. To obtain $T(x,z,t)$ at locations between slices, i.e. $z_{i-1} < z < z_i$, ConOffline uses "delay interpolation", substituting the temperature of the most recent slice to pass through that location. Mathematically, this is given as:

$$T(x,z,t) = T_i(x,t_i(z)) \tag{8}$$

where $t_i(z)$ is found in general by solving the inverse of equation (7). In practice, ConOffline accomplishes this by simply storing the entire temperature history of each slice, and searching through them to find the most recent temperature. An illustration of the delay interpolation result extracted from the slice histories is shown in Figure 1. The approximation error introduced with this procedure at location z at time t is the temperature change at this location from time $t_i(z)$ (most recent "exact estimates") to t, which is a function of the slice spacing. Therefore, the slices are evenly spaced to minimize the approximation error, and the error decays to zero during steady operation.

However, during unsteady casting, the estimation error depends on how many slices (N) ConOffline is managing simultaneously. Obviously, larger N gives higher resolution and more accuracy, but is more computationally intensive. To improve accuracy in this study, ConOffline program was uncoupled from real-time, and the number of slices was increased from 200 (the number of slices managed by CONONLINE for real-time calculation [6]) to 500. In the 15 m long thin-slab caster discussed below, this means a spacing of 0.03 m between slices.

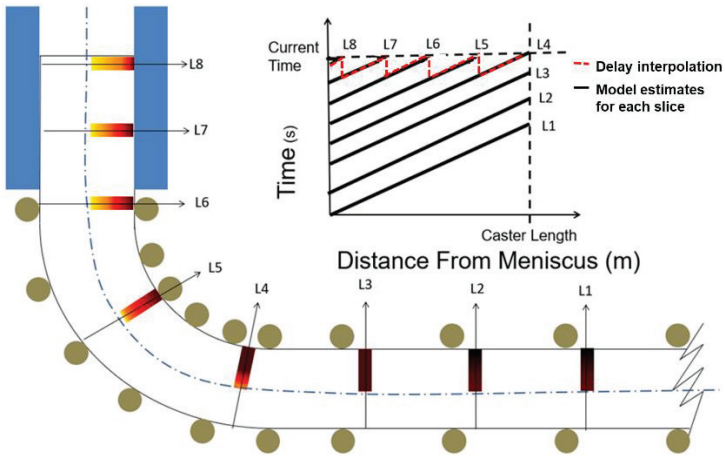

Figure 1. Illustration of ConOffline resolution using 'delay interpolation' method.

CENTERLINE BRIDGING

Using ConOffline, numerical experiments were performed to investigate centerline bridging in a typical commercial caster. This section provides a detailed example.

Casting conditions

Simulations here are based on a thin (90 mm-thick) slab caster at Nucor Steel in Decatur, Alabama. The steel grade simulated is low (0.05 wt-%) Carbon steel, with properties given in Table I. The first case considered is a sudden speed slow-down from 3.5 m/min to 0.5 m/min, with spray water flow rates changed suddenly at the time of the casting speed drop, according to the spray table given in Figure 2.

Table I. Steel properties in simulation

	Value
Liquidus temperature	1532.1 °C
Solidus temperature	1515.3 °C
Pour temperature	1550 °C
Latent heat of solidification	271 kJ/kg

The evolution of metallurgical length with time during the sudden speed drop is shown in Figure 3. The metallurgical length gets shorter, with decreasing rate after $t = 0$ when the speed change begins. At ~180s, there is a sudden drop in metallurgical length. This drop is due to centerline bridging of the liquid core, which is illustrated in the snapshots of the shell thickness profile down the strand in Figure 4. At 60 seconds after the speed drop, the shell thickness no longer increases continuously with distance from the meniscus. The shell at approximately 1.5 m from the meniscus is thinner than both upstream and downstream. This thin spot persists and moves downward with the moving strand. By 187 seconds after the speed drop, the steel is fully solid around 2.17 m, when the two thick spots upstream of the thin spot touch. At the thin spots, there is still liquid further on down the caster. After enough time passes, the liquid in the thin spots solidifies as well, and a final, continuously-increasing profile is reached at 208 seconds after the speed drop, which is the new steady-state profile.

Note in Figure 4 that the small jumps in the shell thickness profile are artifacts of the error due to delay interpolation discussed in Section II. Each jump is at the location of a slice. The error is noticeable because conditions changed drastically in a short period of time. The most recent data, i.e. the points just before each jump in the profile, are the most accurate.

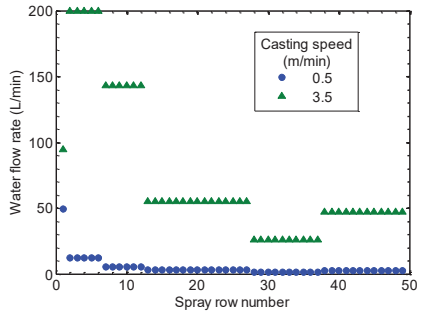

Figure 2. Portion of "spray-table" showing spray water flow rates used at two casting speeds of interest.

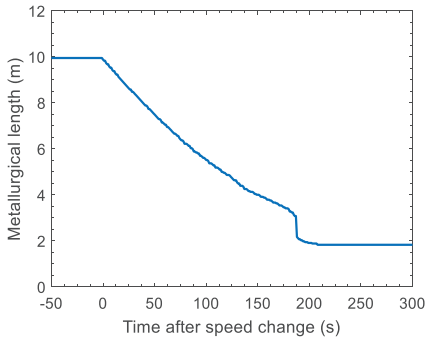

Figure 3. Metallurgical length during sudden speed drop from 3.5 to 0.5 m/min under spray table control.

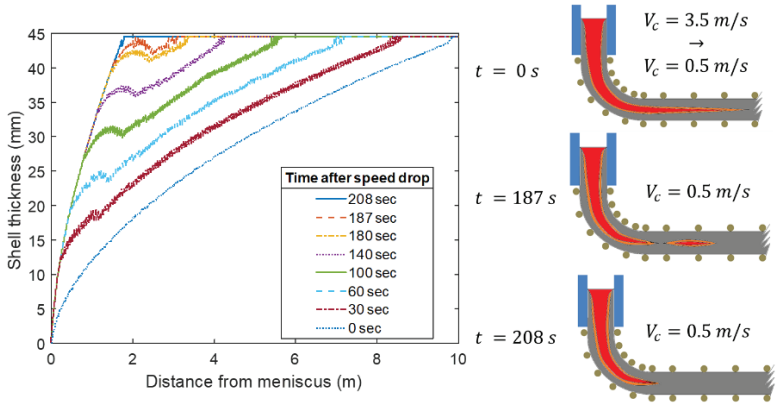

Figure 4. Evolution of shell thickness profile during a sudden speed drop illustrating centerline bridging.

Steps in new bridging mechanism

From Figure 4, a thin spot is observed to develop approximately 1.5 m from the meniscus at 60 seconds after the speed drop. This thin spot persists as solidification proceeds and moves downstream, and it eventually entraps liquid and results in centerline segregation defects in the final product.

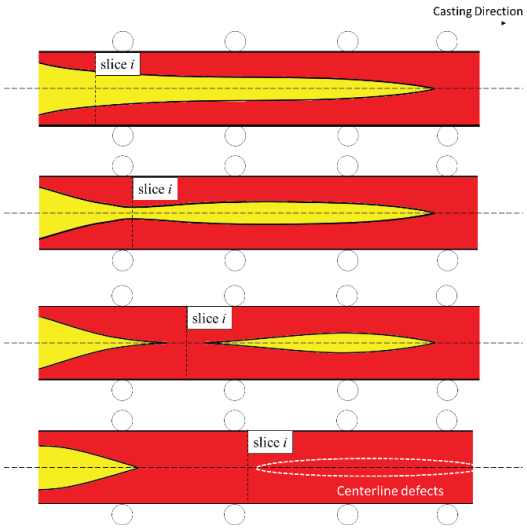

Figure 5. Illustration of steps in centerline bridging after a sudden casting speed drop.

At the time of the speed drop, the spray-water flow rate in each secondary cooling zone drops immediately from the flow rates at 3.0 m/min to the flow rates at 0.5 m/min, according to Figure 2. The heat flux in the mold also drops according to (4). The drop in surface cooling just below the mold is relatively more severe than the heat flux drop near more mold exit. This produces a thin spot in the shell just below mold exit just after the speed drop, and a corresponding thick spot just above that region that solidifies a thicker shell than both upstream and downstream locations, denoted as slice i in Figure 5. The thick spot moves with the strand through secondary cooling, eventually meeting its other half, and entrapping the liquid pocket just below. Eventually, the liquid pocket solidifies, and shrinks, leaving behind a region of centerline segregation and shrinkage cavities just below the bridged region of the strand.

PARAMETRIC STUDIES

In this section, a series of speed drops are simulated with models of a 90 mm caster [14] and a 220 mm caster [9] which were inspired by the Nucor, Decatur thin slab and the JFE thick slab casters respectively. In each test, at time=0, speed dropped

suddenly from v_{c0} and v_{cf}, and spray water flow rates dropped from Q_0 to Q_f. Different tests varied the speed drop, and the initial casting speed. The initial water flow rates Q_0 were taken from caster specific spray tables for the initial casting speed given in Figure 2 for the 90mm caster. In most tests, the final water flow rates were also taken from the caster specific spray tables, but in several tests, these final flow rates were modified.

Effect of speed drop size

Results for the 90 mm caster are given in Figure 6, showing the area of the trapped liquid pocket. Figure 6(a) indicates that for a given initial casting speed, the area of the liquid pocket entrapped by bridging decreases with the extent of the speed drop. Also, for a given speed drop, increasing the initial casting speed causes a decrease in the area of the liquid pocket. This second trend is seen better by replotting the results according to the final casting speed, as shown in Figure 6(b), which shows that the liquid pocket area decreases with increasing final casting speed. In summary, centerline bridging is more severe with larger sudden speed drops, especially when speeds are low.

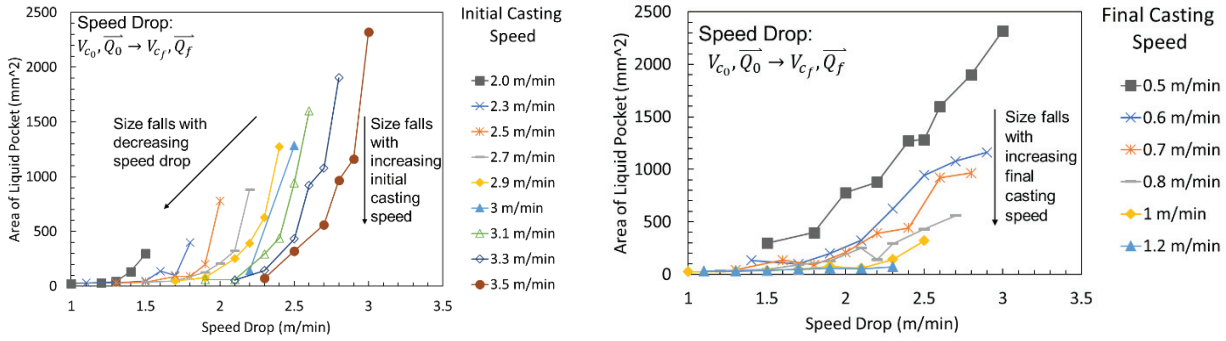

(a) Cases grouped according to initial casting speed

(b) Cases grouped according to final casting speed

Figure 6. Effect of casting speed drop on the area of the entrapped liquid pocket (90 mm thick caster).

Effect of increasing strand thickness

To investigate the effect of strand thickness on this centerline bridging phenomenon, similar tests were conducted for a 220 mm thick-slab caster, inspired by JFE Steel. Details of the caster and spray table are given in [9]. Sample results are shown in Figure 7, which shows similar trends as in Figure 6: the area of the liquid pocket increases with the extent of the speed drop, and with smaller initial and final casting speeds.

Comparing the results in Figure 6 and 7 for the same casting speed conditions (speed drop, initial and final casting speeds), the entrapped liquid pockets are about ten times larger with the 220 mm caster than with the 90 mm caster. Although each caster has its own spray water zones and spray table, so it isn't quite fair to compare these cases, it appears that the bridging mechanism due to casting speed slowdowns causes more severe centerline defects in thicker slab casters.

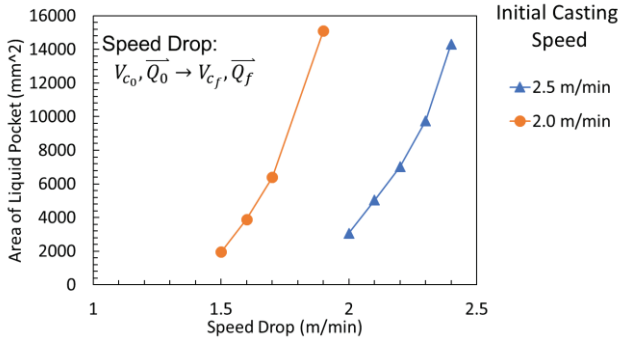

Figure 7. Results of speed drop tests with 220 mm thick slab caster.

Effect of incrementally dropping speed

Considering the drastic increase in the size of the liquid pocket with increasing speed drop, it seemed logical that a more gradual speed drop would lessen the bridging problem. To investigate this idea, two simulations of incremental speed drops were performed for the 90 mm (thin) slab caster. Results are shown in Figure 8.

The first simulation involved dropping speed from 3.5 to 0.5 m/min via speed drops of 1 m/min every 100s. This case was chosen because no bridging was observed for speed drops of this size in previous tests (see Figure 6). As hoped, bridging was completed eliminated, as indicated by the lack of vertical drops in Figure 8(a). This finding is significant, considering that the bridging experienced with the single speed drop from 3.5 to 0.5 m/min produced the worst bridging of all cases in this caster, with an entrapped liquid pocket area of 2300 mm^2.

Considering this success, this same speed drop scenario was repeated using only two speed-drop increments. The first drop was chosen to be the greater, from 3.5 m/min to 1.2 m/min, knowing from results in Figure 6 that drops at higher speeds produce less severe bridging. The second-step speed drop (from 1.2 to 0.5 m/min) of only 0.7 m/min, was expected to decrease bridging severity. The results, given in Figure 8(b), show no bridging, although the crook at ~100 seconds confirms that bridging almost occurred, so this is a borderline case. These results confirm that dropping speed more gradually, such as using a few steps, is able to avoid the bridging phenomenon uncovered in this work. Further work is needed to optimize the speed drops for different casters.

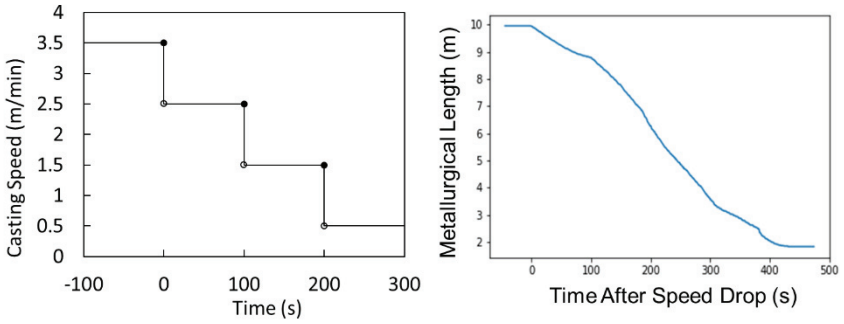

(a) Casting speed drops of 1m/min every 100s from 3.5 m/min to 0.5 m/min.

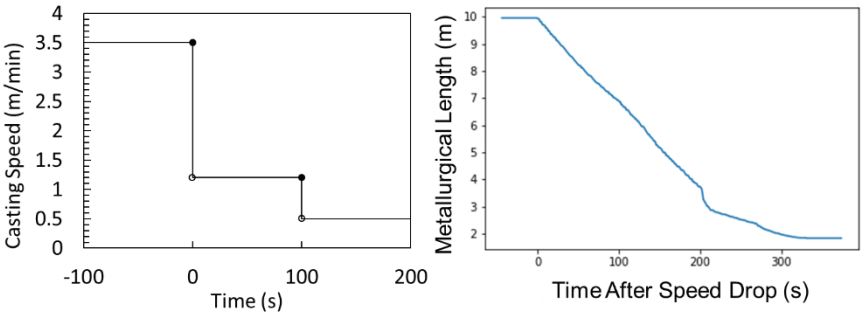

(b) Casting speed drops from 3.5 to 1.2 m/min and to 0.5 m/min after 100s

Figure 8. Simulation results for incremental speed drops (220 mm thick caster with spray table control).

Effects of steel alloy

To investigate the effect of steel alloy composition on the bridging phenomenon, further simulations were conducted to compare two different steel grades: the low carbon steel (0.05wt% C), and a higher alloy steel (0.4 % C, 1.1 % Mn). The results in Figure 9 for the 90-mm thick caster show that the entrapped liquid pockets for the alloy steel are about twice as large and much deeper than that for the low carbon steel under same casting speed and spray-water conditions. This confirms expectations that higher alloying leads to more severe centerline segregation problems from bridging.

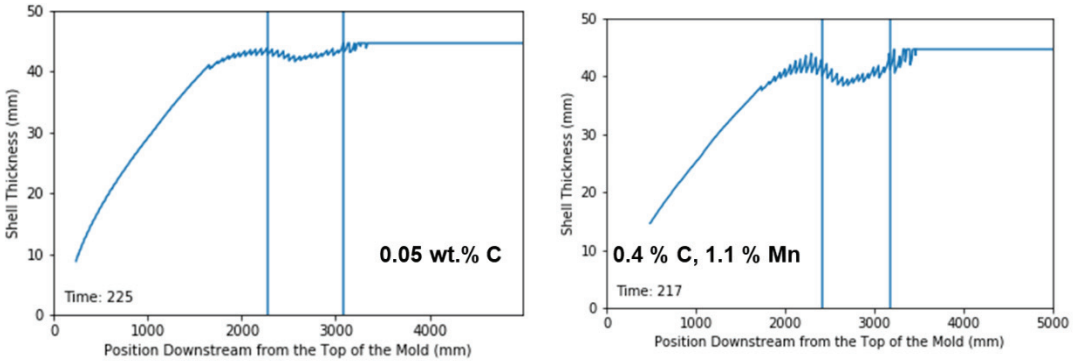

Figure 9. Shell thickness profiles down the caster at the time of maximum bridging (speed drop from 3.5 to 0.5 m/min).

CONCLUSION

This study shows that centerline bridging, leading to centerline segregation and porosity defects, may occur after a sudden drop in casting speed. This is due to a thick spot in the solidifying steel shell forming high in the caster just after the speed drop. The size of the resulting entrapped liquid pocket can be reduced by decreasing the extent of the speed drop, by increasing the initial and final casting speeds, and by decreasing the alloy content. Two strategies to avoid this problem are recommended. First: avoid sudden large speed drops to low casting speeds, opting instead for an incremental or continuous decrease in the casting speed. Second, avoid large drops in spray water flow rates. Instead use dynamic decrease in the spray water flow rates, dropping more gradually towards the steady-state flow rates in the spray table.

ACKNOWLEDGMENT

This work is supported by Continuous Casting Center at Colorado School of Mines, and the National Science Foundation Grant CMMI-13-00907. Special thanks are given to Bryan Petrus, a previous graduate of University of Illinois now working as Process Automation Engineer at Nucor Steel Decatur, for his previous work with CONONLINE to identify the potential for bridging during a speed drop.

REFERENCE

1. J. a. Sirgo, R. Campo, A. López, A. Díaz, and L. Sancho, “Measurement of centerline segregation in steel slabs,” *Conf. Rec. - IAS Annu. Meet. (IEEE Ind. Appl. Soc.*, vol. 1, no. c, pp. 516–520, 2006.

2. M. Miyazaki, K. Isobe, and T. Murao, “Formation mechanism and modeling of centerline segregation,” *Nippon Steel Tech. Rep.*, no. 104, pp. 48–53, 2013.

3. K. Fischer, H. Litterscheidt, W. Rudack, R. Simon, and R. Weber, “Industrial experience gathered in the production of continuously cast slabs,” Thyssen Tech. Berichte, vol. 10, no. 2, pp. 13–18, 1978.

4. T. Murao, T. Kajitani, H. Yamamura, K. Anzai, K. Oikawa, and T. Sawada, “Simulation of the Center-Line Segregation Generated by the Formation of Bridging,” ISIJ Int., vol. 54, no. 2, pp. 359–365, 2014.

5. T. Piccone, T. Natarajan, S. Story, B. Jones, and D. Hreso, “Quantitative Methods for Evaluation of Centerline Segregation,” in AISTech - Iron and Steel Technology Conference Proceedings, 2016.

6. B. Petrus, K. Zheng, X. Zhou, B. G. Thomas, and J. Bentsman, “Real-Time, Model-Based Spray-Cooling Control System for Steel Continuous Casting,” Metall. Mater. Trans. B, vol. 42, no. 1, pp. 87–103, 2011.

7. Y. Meng and B. G. Thomas, “Heat Transfer and Solidification Model of Continuous Slab Casting: CON1D,” Metall. Mater. Trans. B, vol. 34, no. 5, pp. 685–705, 2003.

8. Z. Chen, J. Bentsman, and B. G. Thomas, “Bang-Bang Free Boundary Control of a Stefan Problem for Metallurgical Length Maintenance,” in American Control Conference (ACC) 2018, 2018, pp. 116–121.

9. Z. Chen, J. Bentsman, B. G. Thomas, and A. Matsui, “Study of spray cooling control to maintain metallurgical length during speed drop in steel continuous casting,” *Iron Steel Technol.*, vol. 14, no. 10, pp. 92–103, 2017.

10 B. Santillana, L. C. Hibbeler, B. G. Thomas, A. Hamoen, A. Kamperman, and W. Van Der Knoop, “Heat Transfer in Funnel-mould Casting: Effect of Plate Thickness,” *ISIJ Int.*, vol. 48, no. 10, pp. 1380–1388, 2008.

11. B. Santillana, B. G. Thomas, A. Hamoen, L. C. Hibbeler, A. Kamperman, and W. Van Der Knoop, “Investigation Mould Heat Transfer in Thin Slab Casting with CON1D,” *AISTech 2007 Proc.*, vol. 1, 2007.

12 D. Currey, R. Global, D. Hamilton, and B. G. Thomas, “Utilization of CON1D at ArcelorMittal Dofasco’s No . 2 Continuous Caster for Crater End Determination,” *AISTech - Iron Steel Technol. Conf. Proc.*, vol. I, no. 2, pp. 1177–1186, 2009.

13. H. Shin, B. G. Thomas, G. Lee, J. Park, C. Lee, and S. Kim, “Analysis of Hook Formation Mechanism in Ultra Low Carbon Steel using CON1D Heat Flow – Solidification Model MS & T 2004 Conference Proceedings , (New Orleans , LA), AIST , Warrendale , PA MS & T 2004 Conference Proceedings , (New Orleans , LA), AIST ,” *Mater. Sci. Technol.*, pp. 11–26, 2004.

14. B. Petrus *et al.*, “New Method to Measure Metallurgical Length and Application to Improve Computational Models,” *Iron Steel Technol.*, vol. 12, no. 12, pp. 58–66, 2015.

15. P. Duvvuri, B. Petrus, and B. G. Thomas, “Correlation for Mold Heat Flux Measured in a Thin Slab Casting Mold,” in *AISTech - Iron and Steel Technology Conference Proceedings*, 2014, pp. 2881–2894.

16. T. Nozaki, Jjvi. Matsuno, K. Murata, H. Ooi, and M. Kodama, “A Secondary Cooling Pattern for Preventing Surface Cracks of Continuous Casting Slab,” *Trans. Iron Steel Inst. Jpn.*, vol. 18, no. 6, pp. 330–338, 1978.

